Analysis of the Errors in Polarimetry with Full Poincaré Beams

J. C. Suárez-Bermejo[1], **J. C. González de Sande**[2], **M. Santarsiero**[3], **and G. Piquero**[4]

[1]Materials Science Department, Universidad Politécnica de Madrid, Madrid, Spain
[2]ETSIS de Telecomunicación, Universidad Politécnica de Madrid, Madrid, Spain
[3]Dipartimento di Ingegneria, Universitá Roma Tre, Rome, Italy
[4]Departamento de Óptica, Universidad Complutense de Madrid, 28040 Madrid, Spain

Abstract— The main error sources of a recently proposed Mueller matrix polarimetric method based on the use of full Poincaré beams (FPBs) are described and analysed in detail. Numerical simulations are performed under the presence of different sources of errors. Their influence in the determination of the Mueller matrix is studied for samples presenting either birefringence or diattenuation. The present study will allow to improve the experimental procedure for obtaining the Mueller matrix of a sample using a FPB.

1. INTRODUCTION

During the last decade, polarimetric methods for recovering the Mueller matrix of a sample based on the use of non-uniformly totally polarized (NUTP) beams have been proposed, developed and experimentally tested [1, 2]. Different types of NUTP beams have been considered, including spirally, radially or azimuthally polarized beams, and lately FPBs [3, 4, 5, 6]. A FPB is a field that presents all states of totally polarized light across its transverse section [7, 8, 9]. Several procedures have been developed for synthesizing FPBs (see for example Ref. [9] and references therein). A simple and inexpensive method to obtain a FPB has been recently described [9]. This kind of beam can be used as a parallel polarization state generator for polarimetry, so that the Mueller matrix of a sample can be obtained by measuring the Stokes parameters of the input and output fields at four different positions of the transverse plane [5, 6]. In this contribution a new Mueller matrix polarimetric method based on the use of FPBs [6] will be reviewed. The main sources of error occurring in its experimental implementation will be analysed in detail. In particular, the errors due to an inaccurate positioning of the polarimeter and the errors in the measurement of the Stokes parameters of the input and output fields across their transverse planes will be analysed. The effect of the finite size of the area where the Stokes parameters are measured will also be considered. Results of numerical simulations for several types of samples, such as diattenuators and wave plates, will be presented and discussed. This study will be useful in order to optimize the Mueller matrix measurement with the proposed method.

Besides this Introduction, in Section 2 principles of the Mueller matrix polarimetry based on FPB are briefly reviewed, in Section 3 the main source of errors for this method are analyzed and the results of several numerical simulations of their effects on the determination of the Mueller matrices for samples presenting birrefringence or diattenuation are presented and discussed. The main results are summarized in the Conclusions.

2. REVIEW OF POLARIMETRY WITH A FPB

The polarization state, described by a 4×1 Stokes vector, changes when the light is reflected by or transmitted through a sample. As the used FPB is a non uniformly polarized beam, its Stokes vector depends on the point of the transversal section where it is measured. The Stokes vector $\mathbf{S}^{\text{out}}(r,\theta)$ of the output beam in a given point $\mathbf{r} = (r,\theta)$ of the transverse section is related to the Stokes vector of the input beam in the same point $\mathbf{S}^{\text{in}}(r,\theta)$ through [10]

$$\mathbf{S}^{\text{out}}(r,\theta) = \widehat{M}\,\mathbf{S}^{\text{in}}(r,\theta)\ , \tag{1}$$

where $\widehat{M}$ is the Mueller matrix describing the sample. By measuring the input and output polarization state in four different points $\mathbf{r}_j$, with $j = 0,1,2,3$, of the transverse section of the beam, and arranging such vectors into two 4×4 matrices $\widehat{S}^{\text{out}} = \left(\mathbf{S}^{\text{out}}(\mathbf{r}_0),\ \mathbf{S}^{\text{out}}(\mathbf{r}_1),\ \mathbf{S}^{\text{out}}(\mathbf{r}_2),\ \mathbf{S}^{\text{out}}(\mathbf{r}_3)\right)$

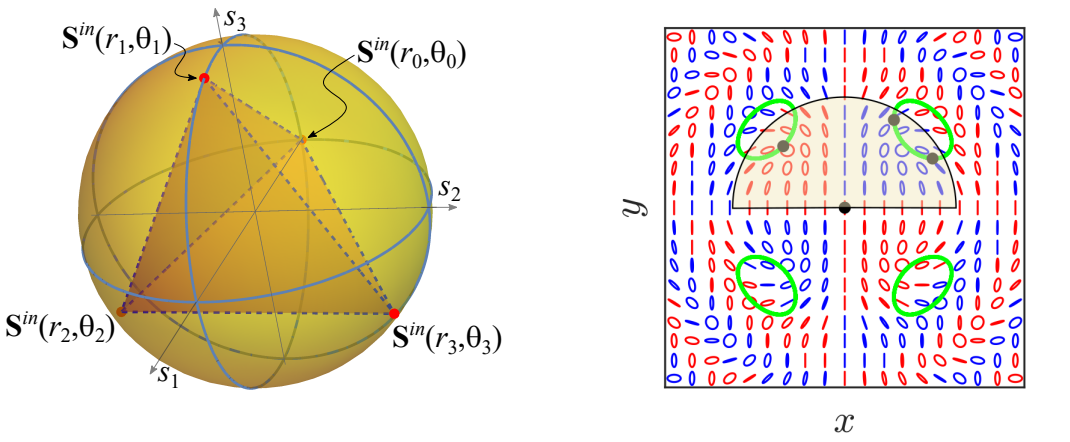

Figure 1: Left: Poincaré sphere showing a possible set of input polarization states for the optimum determination of the Mueller matrix. Right: Polarization pattern of the beam at the output of a uniaxial crystal for an incident beam linearly polarized along y direction. Red (blue) ellipses represent right-handed (left-handed) polarization states. The shaded area maps the whole Poincaré sphere surface. Black dots are a set of points whose polarization states coincide with the vertices of the tetrahedron of the left part. Ovoid green lines are formed when this tetrahedron continuously rotates around s_1 axis.

and $\widehat{S}^{\text{in}} = \left(\mathbf{S}^{\text{in}}(\mathbf{r}_0),\ \mathbf{S}^{\text{in}}(\mathbf{r}_1),\ \mathbf{S}^{\text{in}}(\mathbf{r}_2),\ \mathbf{S}^{\text{in}}(\mathbf{r}_3)\right)$, the Mueller matrix of the sample can be obtained as

$$\widehat{M} = \widehat{S}^{\text{out}} \left(\widehat{S}^{\text{in}}\right)^{-1} , \tag{2}$$

whenever the matrix $\widehat{S}^{\text{in}}$ is invertible. As the input beam is a FPB, it is possible to find different sets of four points in the transverse section of the beam for which $\widehat{S}^{\text{in}}$ is not only invertible, but presents the minimum possible condition number [5, 6, 11]. For any of such sets of points, their polarization states are located at the vertices of a tetrahedron inscribed in the Poincaré sphere (see Fig. 1) [6, 11].

In the present case, the FPB is generated by focusing a laser beam at the entrance face of a uniaxial crystal with its optics axis along the main propagation direction [9]. The field at the output crystal face can be easily calculated assuming certain approximations [12, 9]. The resulting polarization pattern is represented in the right-hand side of Fig. 1. It has been shown that the surface of the Poincaré sphere is mapped in a semicircle with a radius r_M determined by the crystal birefringence [9]. It can be observed that multiple optimum choices (sets of points that minimize the condition number [11]) are possible just by rotating the inscribed tetrahedron. Due to the symmetry of the polarization pattern, all these possibilities are duplicated. The beam can be expanded in such a way that the radius r_M reaches a value of the order of 5 mm.

The polarization state of the FPB before and after inserting the sample under study is measured by a commercial polarimeter with a small pinhole attached at its entrance so the detection area is a small fraction of the radius r_M at the sample plane. The polarimeter is mounted on a XY-micropositioner, so that the pinhole can be centered at the desired positions (as the ones denoted by black dots in the right part of Fig. 1) [5, 6].

3. SOURCES OF ERROR

In order to optimize the Mueller matrix measurement with the proposed experimental method, the main sources of error and their effects need to be analyzed. The most important contributions to the errors in the determination of the Mueller matrix are the following ones (see Fig. 2): in first place, the uncertainties in measurements are related to the precision and accuracy of the commercial light polarimeter that have been used to measure the Stokes parameters of the beam before and after inserting the samples. The second source of error is the possible deviation of the beam after going through the samples. Finally, a third important source or error could be the averaging of

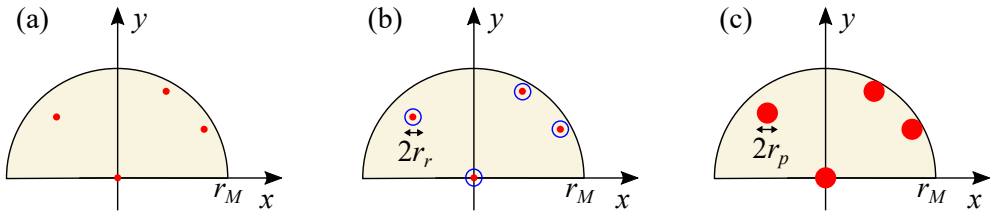

Figure 2: Sources of error. (a) Errors in the Stokes vectors measurement; no error in the positioning a point-like polarimeter is considered, red dots represent the positions in the transverse section of the beam where to measure the Stokes vector of the input and output beam. (b) Error in the positions before and/or after inserting the sample, blue circles represent the maximum deviation from each ideal measurement point; ideal point-like polarimeter with no error in the Stokes measurement is considered. (c) Polarimeter with a circular detection area of radius r_p is considered. Semicircle shaded area represents a region of the transverse section of the FPB where all polarization states can be found.

measurements over a certain integration area of the detector. In the following, these sources of error are taken into account and results of numerical simulations are presented.

Numerical simulations are performed in the following way. The ideal Mueller matrix polarimetry with FPB is simulated by calculating the value of the Stokes parameters at exactly the four optimum measurement points of the beam transverse section (those corresponding to the vertices of the tetrahedron of Fig. 1). Then, a sample represented by a known Mueller matrix $\widehat{M}_T$ is considered and the Stokes vectors at the output of the sample in the four selected points are calculated by using Eq. (1). Obviously, when substituting these sets of input and output Stokes vectors in Eq. (2), exactly the assumed Mueller matrix for the sample is recovered. The real Mueller matrix polarimeter is simulated by adding random white noise of a given amplitude in one of the steps in this process. In this case, the use of Eq. (2) results in a slightly different Mueller matrix $\widehat{M}_S$ than the assumed for the sample $\widehat{M}_T$. In order to represent the errors of the simulated system by a single number, the difference $\delta\widehat{M} = \widehat{M}_S - \widehat{M}_T$ is evaluated and its root mean square defined as

$$\mathrm{rms}\left(\delta\widehat{M}\right) = \frac{1}{4}\sqrt{\sum_{i,j=0}^{3} |\delta M_{ij}|^2}\,, \tag{3}$$

is evaluated. This process is repeated a given number of times N_S for each value of the considered parameters. Results of numerical simulations for several types of samples, such as diattenuators and wave plates, will be presented.

3.1. Stokes vectors measurement errors

In this case, only the errors in the measurement of the Stokes vectors are considered (see Fig. 2 (a)). These are due to the inaccuracy of the commercial Stokes polarimeter employed to determine the state of polarization at the measurement points. After calculating the Stokes vectors in the four selected points for the input FPB and for the output beam after inserting the sample (represented by a known Mueller matrix $\widehat{M}_T$), a random white noise with amplitude ϵ is added to the normalized Stokes parameters $\mathbf{S}^{\mathrm{in}}(r_i,\theta_i)/S_0^{\mathrm{in}}(r_i,\theta_i)$ and $\mathbf{S}^{\mathrm{out}}(r_i,\theta_i)/S_0^{\mathrm{out}}(r_i,\theta_i)$. These noisy Stokes vectors are then substituted in Eq. (2) to obtain a simulated experimental Mueller matrix of the sample $\widehat{M}_S$. Finally, the rms value of the difference $\widehat{M}_S - \widehat{M}_T$ is calculated. This process is repeated N_S =1000 times for each value of maximum amplitude ϵ of the added white noise.

Figure 3 shows the results for ideal wave plates (WP) and ideal linear depolarizers (LP). The results are practically the same for a quarter-wave plate (QWP) than for a half-wave plate (HWP). The simulations were carried out for different values of the WP retardance and similar results than those shown in Fig. 3 were obtained. These simulations were repeated for multiple values of the orientation of the fast axis of the WP and any significant variation was found. It can be observed that rms $\left(\delta\widehat{M}\right)$ values are slightly lower for the case of ideal LP. For this latter case, a very small

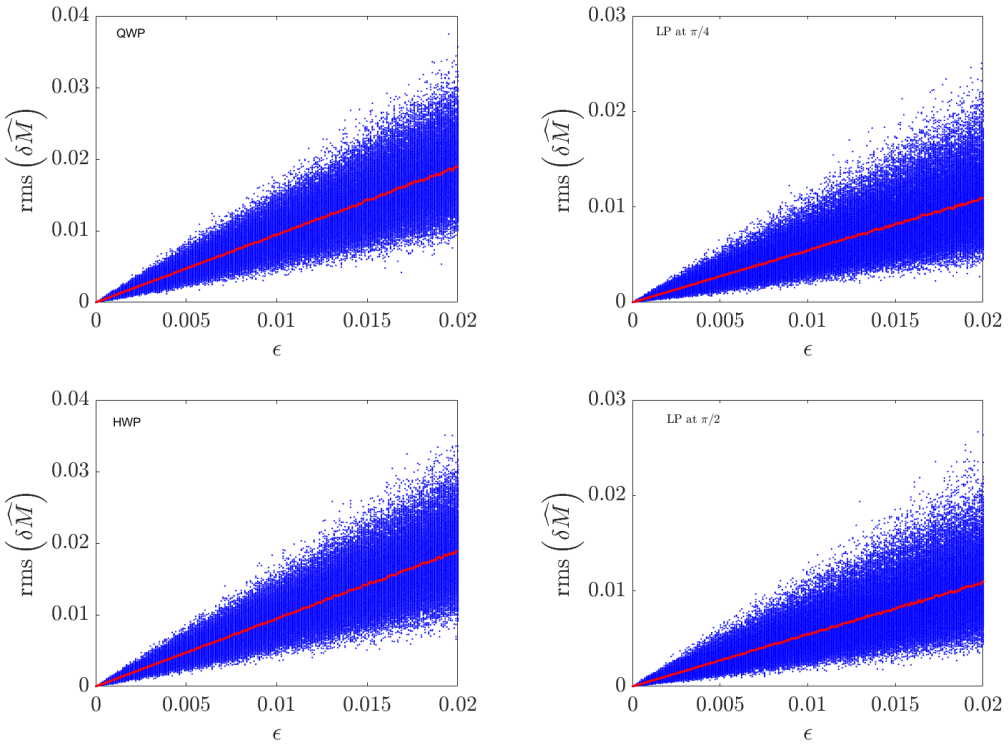

Figure 3: Root mean square of the difference between the Mueller matrix obtained from simulated measurements and the actual one. Red lines represent the average value of the N_S simulations done for each value of the maximum amplitude of the added white noise.

variation of the rms $\left(\delta\widehat{M}\right)$ is observed with the rotation of the transmission axis of the LP.

3.2. Inaccurate position measurement

Positioning of the pinhole in the exact places where the 4 optimum polarization states for measuring the Stokes parameters are located is not strictly necessary. The only effect of small mispositioning is that Stokes vectors of the input beam are not exaclty on the vertices of the tetrahedron shown in Fig. 1. Then, the condition number of matrix $\widehat{S}^{\text{in}}$ is slightly higher than the minimum one and the upper bound for errors of the measured Mueller matrix is higher. However, the Stokes vectors of the input beam and the output beam should be measured at the same positions.

Small deviations of the beam or changes in the position of the polarimeter between the measurement of the input and output beam Stokes vectors is an important source of error in the described method. To evalute its influence on the Mueller matrix measurement, it is considered that the Stokes vectors are measured without error. The input beam state of polarization is calculated at exactly the four positions indicated by red dots in Fig. 2 (b). However, for the output beam, the Stokes vector is evaluated in points randomly distributed inside a small circle of radius r_r centered in each of the four positions. The radius r_r of this small circle is selected as a fraction of the radius r_M. The Mueller matrix of the sample is obtained by means of Eq. (2) using the output Stokes vectors at such inaccurate positions. Then, the difference between the calculated matrix and the one assumed for the sample is evaluated and its rms evaluated. This process is repeated $N_S = 1000$ times for each set of values of the rest of parameters.

The results of such simulations are shown in Fig. 4 for the case of phase plate versus the radius of the position mismatch (r_r) between the measurement of the Stokes vector for the input and output beam. Left part of Fig. 4 shows that the rms of the differences grows linearly with increasing r_r/r_M ratio. The results are shown only for a QWP, but similar results are found for any retardance value of the WP. The right side of this figure shows that these results are independent on the WP fast axis orientation.

Figure 5 shows the results of the simulations for the case of linear diattenuators when two different radius of the position mismatch (r_r) are considered. The results are presented as a function of the transmission axis orientation ϕ of the diattenuator for several values of the diattenuation.

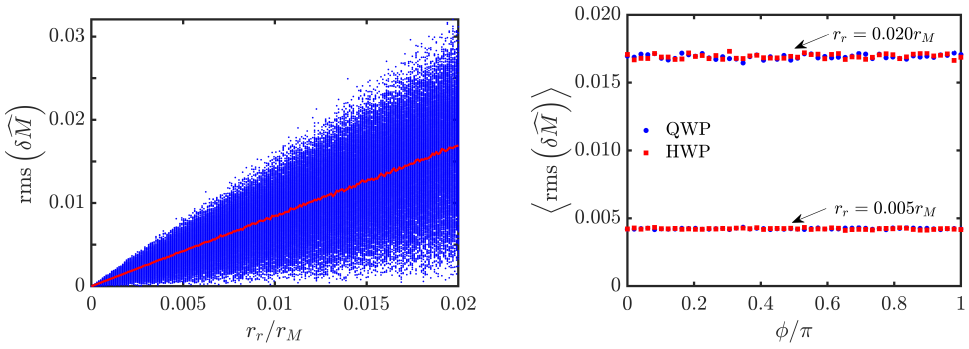

Figure 4: Left: Root mean square of the difference between the Mueller matrix obtained from simulated measurements and the actual one; red line represents the average value of the N_S simulations done for each value of r_r/r_M ratio for a QWP. Right: Mean value of the rms of $\delta\widehat{M}$ for two values of the r_r/r_M ratio for a ideal QWP and a ideal HWP as a function of the orientation of its fast axis relative to the x direction.

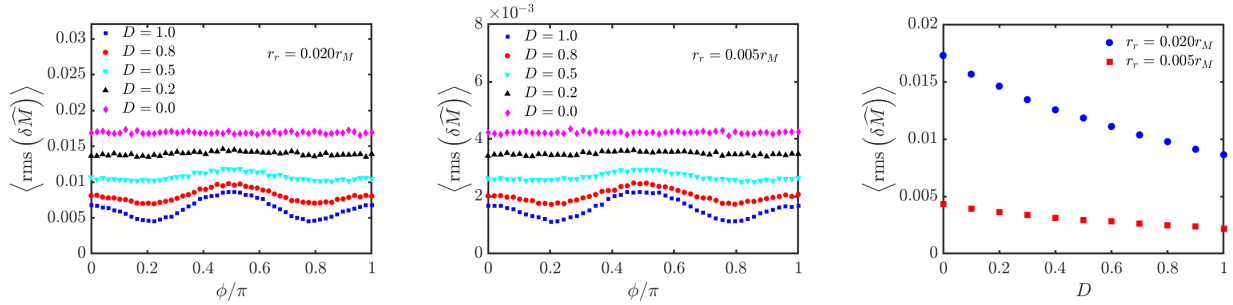

Figure 5: Mean of the rms of the difference between the Mueller matrix obtained from simulated measurements and the actual one versus the linear diattenuator orientation for several values of the diattenuation for several values of the diattenuation and two values of radius r_r. Right graph shows the largest value of the of $\left\langle \text{rms}\left(\delta\widehat{M}\right)\right\rangle$ as a function of the diattenuation.

Only the mean value of $\text{rms}\left(\delta\widehat{M}\right)$ after $N_S = 1000$ simulations for each value of the transmission axis orientation and diattenuation value is shown for better visualization of the observed differencies. The diattenuation is defined as [13]

$$D = \frac{I_{max} - I_{min}}{I_{max} + I_{min}}, \tag{4}$$

where I_{max} (I_{min}) is the maximum (minimum) transmitted intensity by the diattenuator, when the input polarization state is varied over all possibles polarization states. For ideal linear polarizer, this parameter reaches its maximum possible value $D = 1$, and takes the value $D = 0$ when the sample does not present diattenuation. When the diattenuation value is close to 1, there is a dependence of the expected errors with the orientation of the diattenuator. On the other hand, it can be observed that the expected errors in the determination of the Mueller matrix with the proposed method is lower for ideal polarizer than for samples without diattenuation. The right part of the Fig. 5 clearly shows this result.

3.3. Averaging over a finite size area

The last source of error that is considered is the finite size area where the Stokes parameters are measured (see Fig. 2 (c)). Since the polarization state varies across the beam section of the FPB, a small pinhole can be used to obtain a uniform polarization in the measured region, but the pinhole radius should be as large as possible to ensure high power and good signal-to-noise ratio. For a pinhole radius r_p (expressed as a fraction of the distance r_M) the measured Stokes vector at each point is evaluated as the spatial average [14] over a circular region of radius r_p and centered at the ideal measurement points (see Fig. 2 (a)).

When simulating this situation, the same average is done for the Stokes vector of the input and output beams. Then, the use of Eq. 2 gives exactly the same Mueller matrix as that assumed for

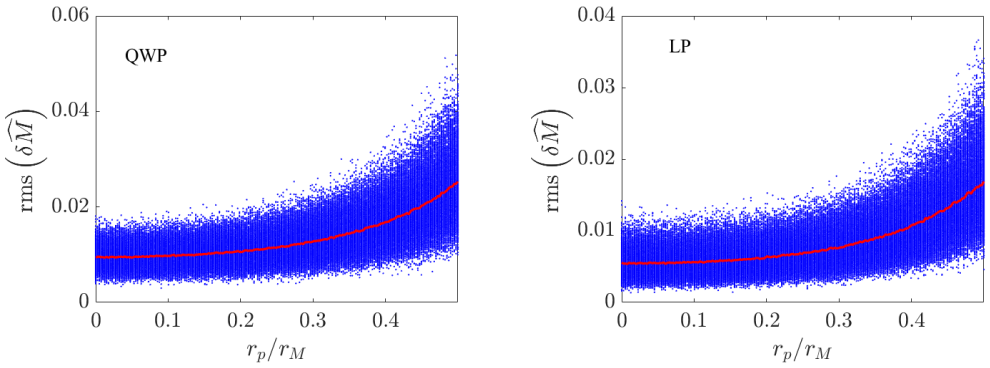

Figure 6: Root mean square of the difference matrix $\delta\widehat{M}$ for $\epsilon = 0.01$. Red line shows the mean value.

the sample. This implies that the average over a finite area does not produce any error in the determination of the sample's Mueller matrix.

The effect of considering finite size area can only be noticed in the presence of other source of error. This is due to the fact that the average of the states of polarization reduces the degree of polarization in each measured region. Then, the measured states of polarization does not lie on the vertices of the tetrahedron shown in Fig. 1, but inside the Poincaré sphere, so that the condition number of $\widehat{S}^{in}$ grows and the upper bound of the errors also grows.

To show this effect, a simulation has been carried out by considering an error of maximum amplitude ϵ in the measured normalized Stokes vectors and a finite radius r_p of the detection area. Figure 6 shows the result of such a simulation for a QWP (the results are similar for any retardance and any orientation of its fast axis) and for a linear polarizer ($D = 1$) with transmission axis along y axis (which is the worst case for this element). It can be observed that the expected error is nearly constant for r_p/r_M up to 0.10. For higher ratios the errors grow at an increasing rate with increasing r_p/r_M ratio.

4. CONCLUSION

The main sources of error when determining the Mueller matrix of a sample by means of a FPB have been identified and their effects have been studied. Simulations show that the most important sources of error are the inaccuracy in the measurement of the Stokes vectors and possible deviation of the beam or inaccurate positioning of the polarimeter between the two measurements (before and after inserting the sample) of the Stokes vectors in the four selected points. It has been shown that the effect of measuring the Stokes vectors in an extended area can be neglected if this area is small compared with the area of the transverse section of the beam where all possible states of polarization can be found ($r_p < 0.1 r_M$). For a given accuracy of the polarimeter, the beam can be expanded in such a way that the possible beam deviations and inaccurate positioning of the polarimeter introduces an error below to that due to the limited polarimeter accuracy.

ACKNOWLEDGMENT

This work has been partially supported by Spanish Ministerio de Economía y Competitividad under project FIS2016-75147.

REFERENCES

1. Tripathi, S. and K. C. Toussaint, "Rapid Mueller matrix polarimetry based on parallelized polarization state generation and detection," *Opt. Express*, Vol. 17, No. 24, 21396–21407, 2009.
2. Töppel, F., A. Aiello, C. Marquardt, E. Giacobino and G. Leuchs, "Classical entanglement in polarization metrology," *New J of Phys*, Vol. 16, No. 7, 073019, 2014.
3. de Sande, J. C. G., M. Santarsiero and G. Piquero, "Spirally polarized beams for polarimetry measurements of deterministic and homogeneous samples," *Opt Laser Eng*, Vol. 91, 97 – 105, 2017.
4. de Sande, J. C. G., G. Piquero and M. Santarsiero, "Polarimetry with azimuthally polarized light," *Opt Commun*, Vol. 410, 961 – 965, 2018.

5. de Sande, J. C. G., G. Piquero and M. Santarsiero, Polarimetry with non-uniformly polarized beams, *Proceedings of Trends in Electromagnetic Coherence*, Joensuu, Finland, June 2018, 76–77.
6. Suárez-Bermejo, J. C., J. C. G. de Sande, M. Santarsiero and G. Piquero, Mueller Matrix Polarimetry Using Full Poincar Beams, (submitted).
7. Beckley, A. M., T. G. Brown and M. A. Alonso, "Full Poincaré beams," *Opt Express*, Vol. 18, No. 10, 10777–10785, 2010.
8. Galvez, E. J., S. Khadka, W. H. Schubert and S. Nomoto, "Poincaré-beam patterns produced by nonseparable superpositions of Laguerre-Gauss and polarization modes of light," *Appl Opt*, Vol. 51, No. 15, 2925–2934, 2012.
9. Piquero, G. , L. Monroy, M. Santarsiero, M. Alonzo and J. C. G. de Sande, "Synthesis of full Poincaré beams by means of uniaxial crystals," *J Opt*, Vol. 20, No. 6, 065602(1–6) , 2018.
10. Goldstein, D. H., *Polarized Light,* Marcel Dekker, Inc., New York, 2003.
11. Layden, D., M. F. G. Wood and I. A. Vitkin, "Optimum selection of input polarization states in determining the sample Mueller matrix: a dual photoelastic polarimeter approach," *Opt Express*, Vol. 20, No. 18, 20466–20481, 2012.
12. Piquero, G. and J. Vargas-Balbuena, "Non-uniformly polarized beams across their transverse profiles: an introductory study for undergraduate optics courses," *Eur J Phys*, Vol. 25, No. 6, 793–800, 2004.
13. Chipman, R. A., Polarimetry, 3rd Edition, Vol. I, McGraw-Hill Companies, 2010, Ch. 15, pp. 1 – 46.
14. G. Piquero, J. M. Movilla, P. M. Mejías, R. Martínez-herrero, "Degree of polarization of non-uniformly partially polarized beams: a proposal," *Opt Quant Electron*, Vol. 31, No. 3, 223–226, 1999.